Supporting Information

Paramagnetic One-dimensional Chain Containing High-spin Manganese Atoms Showing Antiferromagnetic Interaction Through –Pt–Rh–Rh–Pt– Bonds

Kazuhiro Uemura,* Yusuke Aoki, and Atsushi Takamori

Department of Chemistry and Biomolecular Science, Faculty of Engineering, Gifu University, Yanagido 1-1, Gifu, 501-1193, Japan
* E-mail: k_uemura@gifu-u.ac.jp

Contents

Analyses of magnetic susceptibility measurements.

Fitting to the results of magnetic susceptibility measurements for $[Pt_2Mn(piam)_4(NH_3)_4](PF_6)_2$ (**1**) and $[\{Rh_2(O_2CCH_3)_4\}\{Pt_2Mn(piam)_4(NH_3)_4\}]_n(PF_6)_{2n}\cdot 1.5n$EtOH (**2**) were shown with Figures S14–S21. Table S6 summarizes the J values (cm^{-1}) and distances (Å) of Mn---Mn in reported 1D compounds.

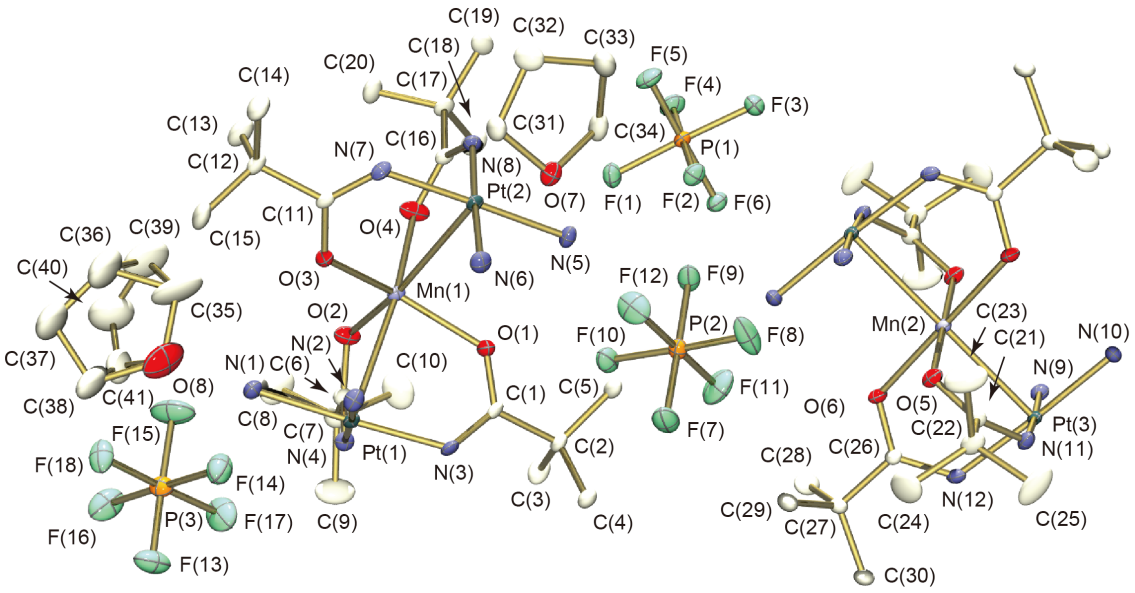

Figure S1. Crystal structure of $[Pt_2Mn(piam)_4(NH_3)_4]_3(PF_6)_6 \cdot 4THF$ (**1·THF**). The hydrogen atoms are omitted for clarity.

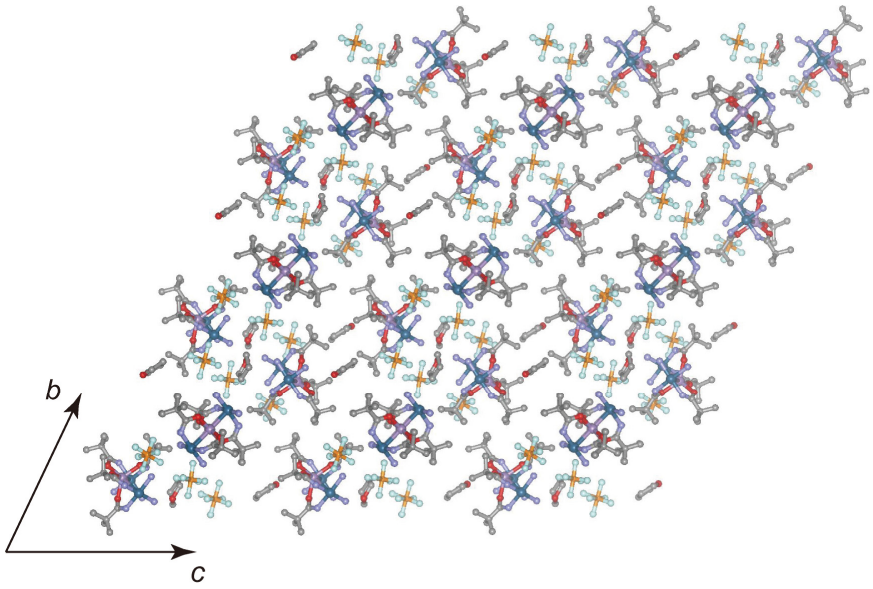

Figure S2. Crystal packing of $[Pt_2Mn(piam)_4(NH_3)_4]_3(PF_6)_6 \cdot 4THF$ (**1·THF**). The hydrogen atoms are omitted for clarity.

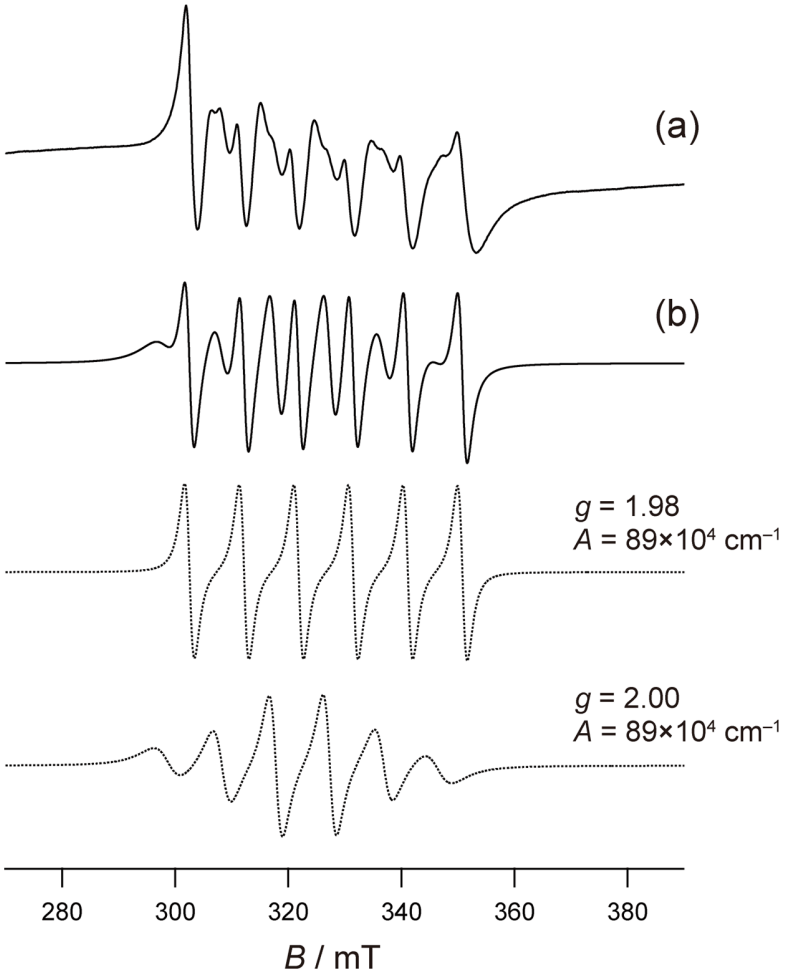

Figure S3. (a) Continuous wave EPR spectrum of $[Pt_2Mn(piam)_4(NH_3)_4](PF_6)_2$ (**1**) in MeOH and (b) its simulation which is sum of two spectra (dotted lines) calculated with *g* and *A* values.

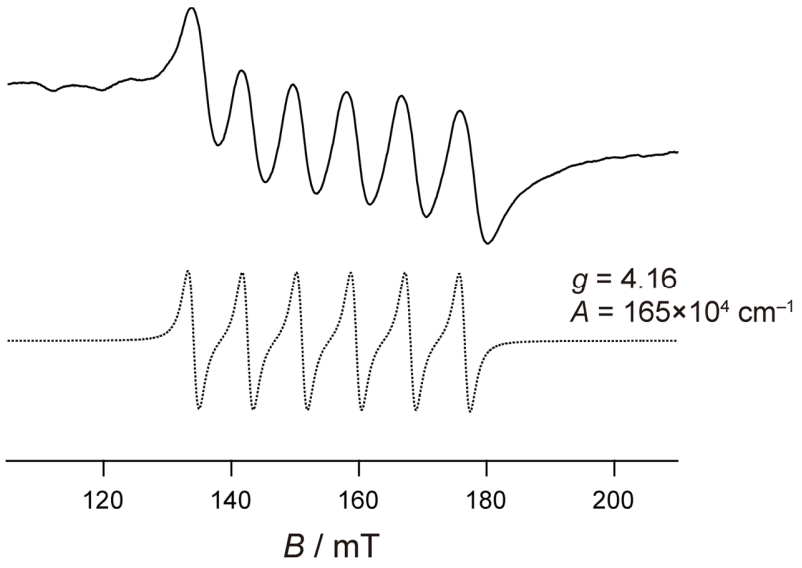

Figure S4. Continuous wave EPR spectrum of $[Pt_2Mn(piam)_4(NH_3)_4](PF_6)_2$ (**1**) in THF and its simulation (dotted lines) calculated with *g* and *A* values.

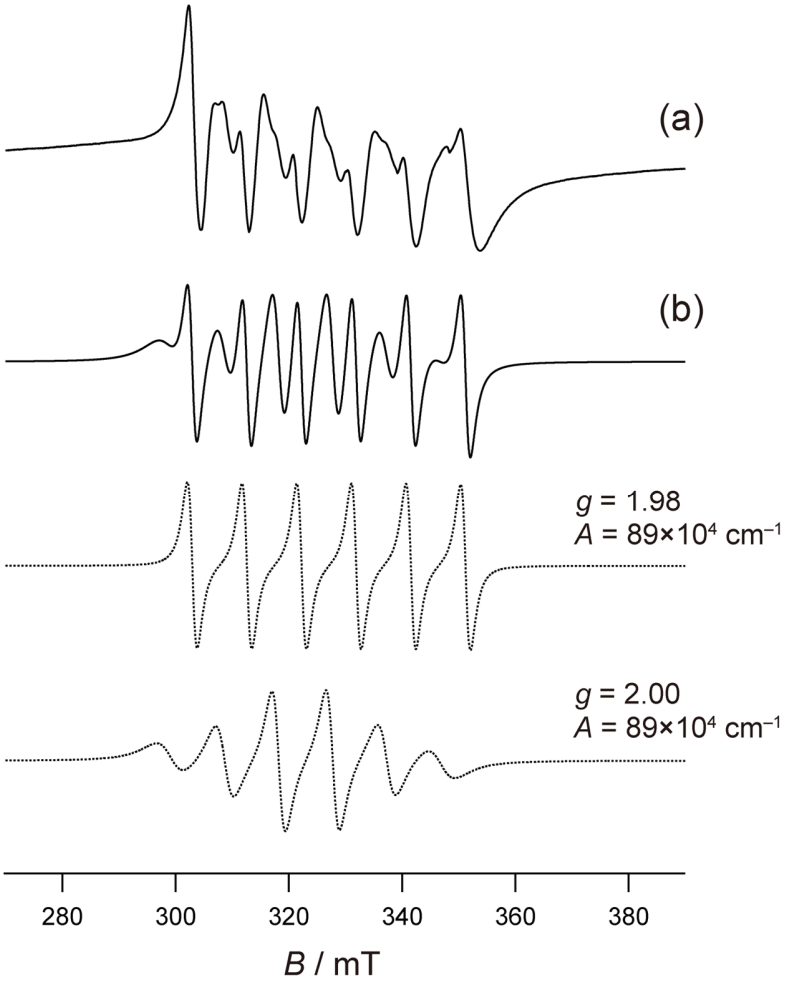

Figure S5. (a) Continuous wave EPR spectrum of $[Pt_2Mn(piam)_4(NH_3)_4](PF_6)_2$ (**1**) in MeCN and (b) its simulation which is sum of two spectra (dotted lines) calculated with *g* and *A* values.

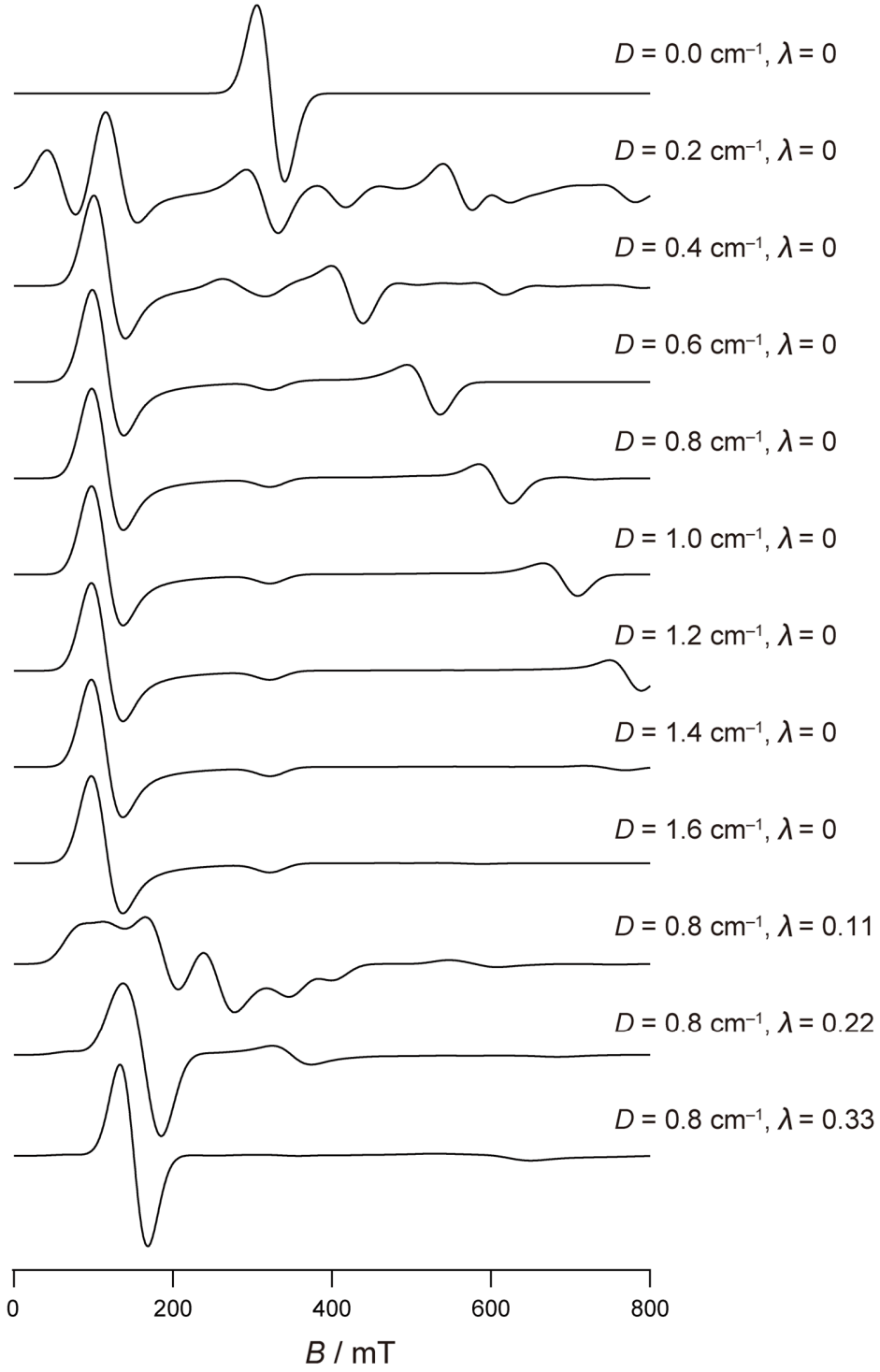

Figure S6. EPR simulation calculated with several ZFS parameters D and λ (= E/D) using EasySpin software. Calculation settings: microwave frequency, 9.05 GHz; g = 2.0; S = 5/2; peak-to-peak width, 35 mT.

Table S1. Optimized coordinates for $[Pt_2Mn(NHCOCH_3)_4(NH_3)_4]^{2+}$ ($\mathbf{1_{Td}}$).

1	Pt	2.5164339	-0.610865	0.2322675
2	Pt	-2.4828216	-0.6357774	-0.2590072
3	Mn	-0.0754583	0.9199576	-0.0453833
4	O	-0.3156406	0.1677249	1.916481
5	O	-1.5606061	2.3467415	-0.2368554
6	O	0.2530128	0.0617175	-1.9182685
7	N	2.559477	-0.5579976	2.291542
8	H	3.1779369	0.1949714	2.6004169
9	H	2.8509739	-1.398618	2.7905578
10	H	1.6075509	-0.300243	2.5896871
11	N	-2.7235859	-0.1374231	-2.2480642
12	H	-3.2311784	0.7471097	-2.3161048
13	H	-3.231692	-0.8041912	-2.8304169
14	H	-1.7911053	0.0196489	-2.6503842
15	N	2.444179	-0.5462149	-1.7773262
16	H	3.3039924	-0.6373814	-2.3080297
17	N	3.2724159	1.2606291	0.2293579
18	H	4.2834377	1.3473597	0.222526
19	N	-3.3655776	1.1235546	0.2847462
20	H	-4.3058804	1.1224048	0.6629141
21	O	1.3477147	2.3805517	0.0330905
22	N	1.8154658	-2.5911145	0.2552841
23	H	1.6340637	-2.9121899	-0.6964401
24	H	0.9664731	-2.7145779	0.8055519
25	H	2.5143505	-3.2340014	0.6346402
26	N	-1.6597372	-2.4275354	-0.9065452
27	H	-2.2945632	-2.9672508	-1.4983692
28	H	-1.4174844	-3.0418749	-0.1288871
29	H	-0.8169809	-2.2318892	-1.4497025
30	N	-2.2083853	-1.0287959	1.734089
31	H	-2.967562	-1.4585002	2.2523676
32	C	-2.7541847	2.2914218	0.1806934
33	C	-1.2756736	-0.4657076	2.466322
34	C	1.3938584	-0.1625635	-2.4768329
35	C	1.4966099	0.0196559	-3.9700426
36	H	1.3172479	1.0726576	-4.2091833
37	H	0.7176045	-0.5628243	-4.4701904
38	H	2.4679114	-0.2726711	-4.3721224
39	C	2.6033798	2.390913	0.1018675
40	C	3.3310766	3.7099665	0.0491321
41	H	3.0887679	4.2087113	-0.893436
42	H	4.4143792	3.6107488	0.1357959
43	H	2.9607366	4.3496963	0.8547092
44	C	-1.3147141	-0.5605811	3.9720394
45	H	-0.3698682	-0.9609978	4.3507522
46	H	-2.1321891	-1.1821495	4.3406849
47	H	-1.4237593	0.4475205	4.3835991
48	C	-3.4679006	3.5696164	0.537067
49	H	-4.501105	3.4134408	0.8516996
50	H	-3.4509504	4.2374546	-0.3286313
51	H	-2.9167374	4.070872	1.3376382

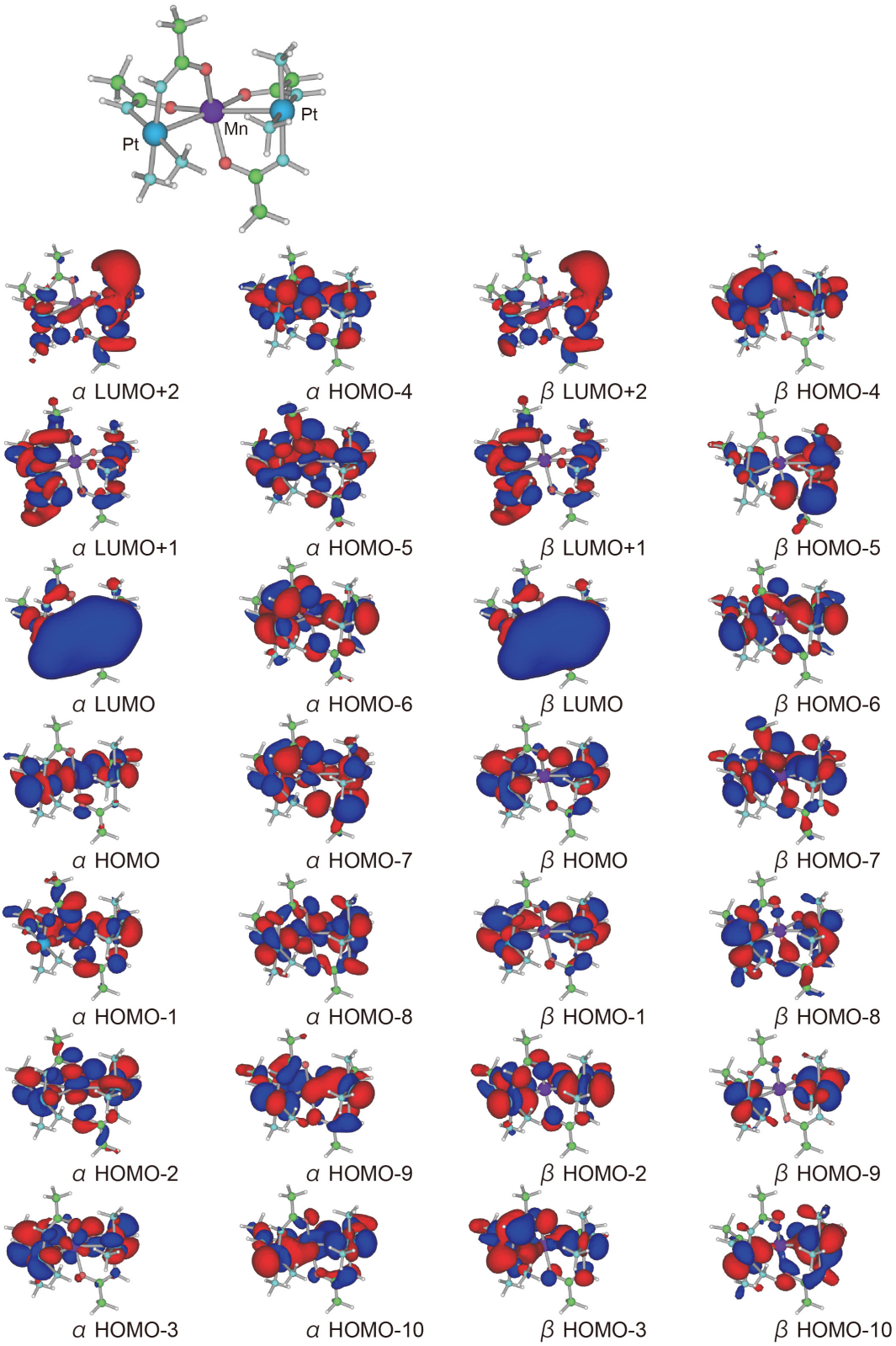

Figure S7. Result of DFT calculation of $[Pt_2Mn(NHCOCH_3)_4(NH_3)_4]^{2+}$ ($\mathbf{1_{Td}}$).

Table S2. Optimized coordinates for $[Pt_2Mn(NHCOCH_3)_4(NH_3)_4]^{2+}$ (**1_{Oh}**).

1	Pt	0.5651936	2.4394414	0.8244129
2	Mn	0	0	0
3	O	1.3102786	-0.5878122	1.5708449
4	O	1.6962623	0.2602686	-1.2897845
5	N	2.2893548	2.1825913	-0.2129645
6	H	3.0595875	2.8218738	-0.0511726
7	N	1.3417562	1.5225952	2.4294202
8	H	1.6998781	2.0787397	3.1986141
9	N	-0.2711771	3.2738209	-0.8515967
10	H	0.4615116	3.5562184	-1.5059056
11	H	-0.8511077	4.1008763	-0.7012793
12	H	-0.8410948	2.5632878	-1.3369157
13	N	-1.2037076	2.5896601	1.8729279
14	H	-1.6704882	1.6684662	1.8367771
15	H	-1.8718094	3.2900682	1.5497821
16	H	-1.0337393	2.7892233	2.8603731
17	C	2.5544415	1.1755213	-1.0359282
18	C	1.6305576	0.2290096	2.5014768
19	C	3.9008607	1.1004929	-1.7134442
20	H	4.4138265	0.1885888	-1.3928041
21	H	4.5416464	1.9565069	-1.4960455
22	H	3.7554261	1.0315045	-2.7950334
23	C	2.3525087	-0.3113436	3.7105526
24	H	1.742983	-1.0893373	4.1791134
25	H	2.5796527	0.4534042	4.4550279
26	H	3.2880494	-0.7777125	3.3879932
27	Pt	-0.5651936	-2.4394414	-0.8244129
28	O	-1.3102786	0.5878122	-1.5708449
29	O	-1.6962623	-0.2602686	1.2897845
30	N	-2.2893548	-2.1825913	0.2129645
31	H	-3.0595875	-2.8218738	0.0511726
32	N	-1.3417562	-1.5225952	-2.4294202
33	H	-1.6998781	-2.0787397	-3.1986141
34	N	0.2711771	-3.2738209	0.8515967
35	H	-0.4615116	-3.5562184	1.5059056
36	H	0.8511077	-4.1008763	0.7012793
37	H	0.8410948	-2.5632878	1.3369157
38	N	1.2037076	-2.5896601	-1.8729279
39	H	1.6704882	-1.6684662	-1.8367771
40	H	1.8718094	-3.2900682	-1.5497821
41	H	1.0337393	-2.7892233	-2.8603731
42	C	-2.5544415	-1.1755213	1.0359282
43	C	-1.6305576	-0.2290096	-2.5014768
44	C	-3.9008607	-1.1004929	1.7134442
45	H	-4.4138265	-0.1885888	1.3928041
46	H	-4.5416464	-1.9565069	1.4960455
47	H	-3.7554261	-1.0315045	2.7950334
48	C	-2.3525087	0.3113436	-3.7105526
49	H	-1.742983	1.0893373	-4.1791134
50	H	-2.5796527	-0.4534042	-4.4550279
51	H	-3.2880494	0.7777125	-3.3879932

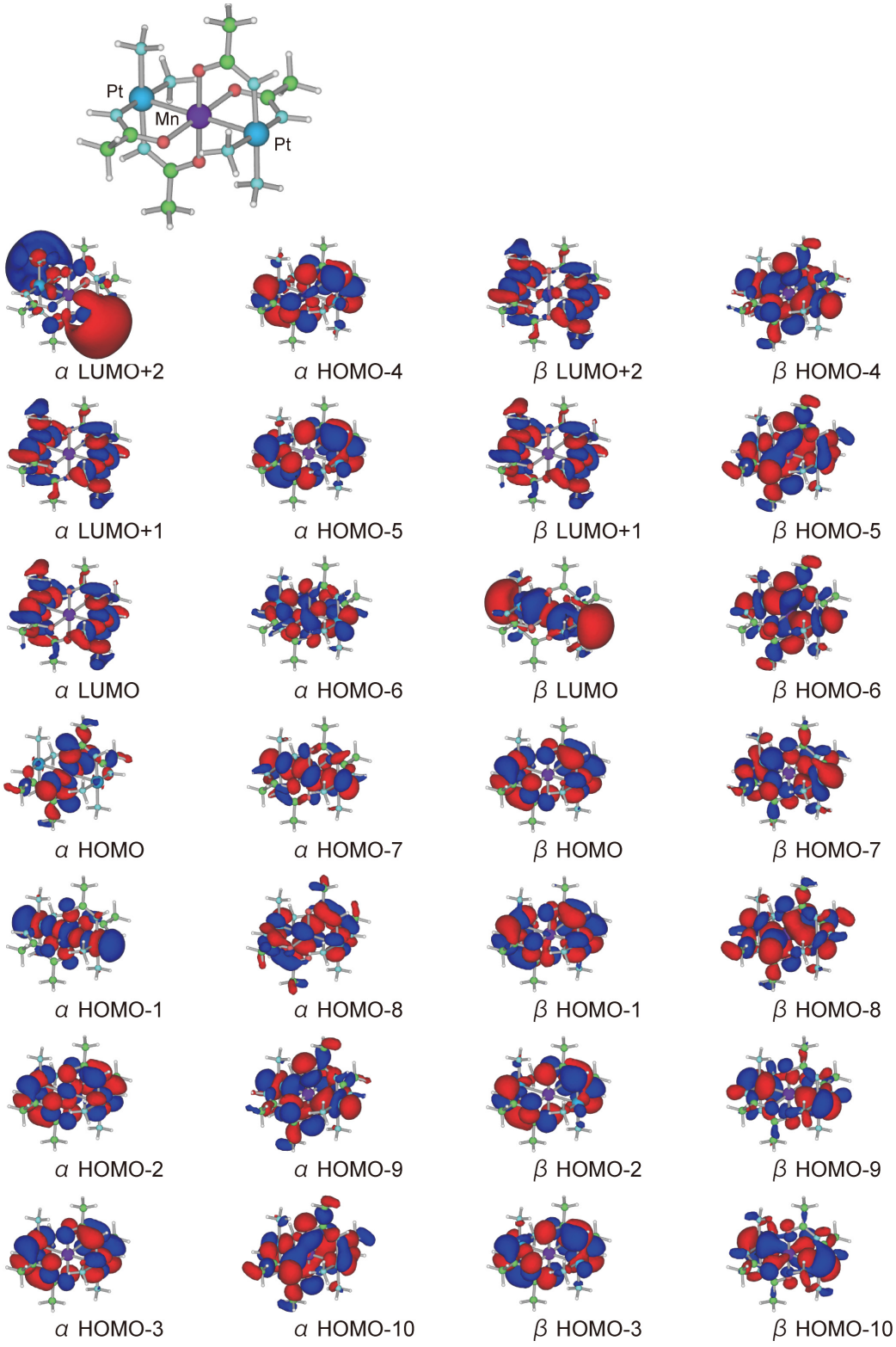

Figure S8. Result of DFT calculation of $[Pt_2Mn(NHCOCH_3)_4(NH_3)_4]^{2+}$ (**1**$_{Oh}$).

Table S3. Comparison of selected distances (Å) and angles (°) between two kinds of trinuclear complex in $[Pt_2Mn(piam)_4(NH_3)_4]_3(PF_6)_6 \cdot 4THF$ (**1·THF**), $[Pt_2Mn(NHCOCH_3)_4(NH_3)_4]^{2+}$ ($\mathbf{1_{Td}}$), and $[Pt_2Mn(NHCOCH_3)_4(NH_3)_4]^{2+}$ ($\mathbf{1_{Oh}}$).

Compounds	Pt–Mn (Å)	Pt–Mn–Pt (°)	Mn–O (Å) O–Mn–O (°)
1·THF	2.8639(8), 3.0176(8)	116.93(3)	2.093(4), 2.076(4), 2.108(4), 2.032(4) 89.83(17), 107.61(17), 103.69(17), 101.82(18), 109.14(17), 135.47(17)
$\mathbf{1_{Td}}$	2.8743, 3.0230	116.7985	2.0683, 2.0862, 2.1148, 2.0408 104.4595, 134.7793, 107.3434, 108.2844, 90.6067, 102.6592
1·THF	2.62666(18)	180	2.117(4), 2.132(4), 2.117(4), 2.132(4) 180, 90.27(16), 89.73(16), 89.73(16), 90.27(16), 180
$\mathbf{1_{Oh}}$	2.6363	180	2.1468, 2.1284, 2.1468, 2.1284 89.4541, 90.5459, 180, 89.4541, 180, 90.5459

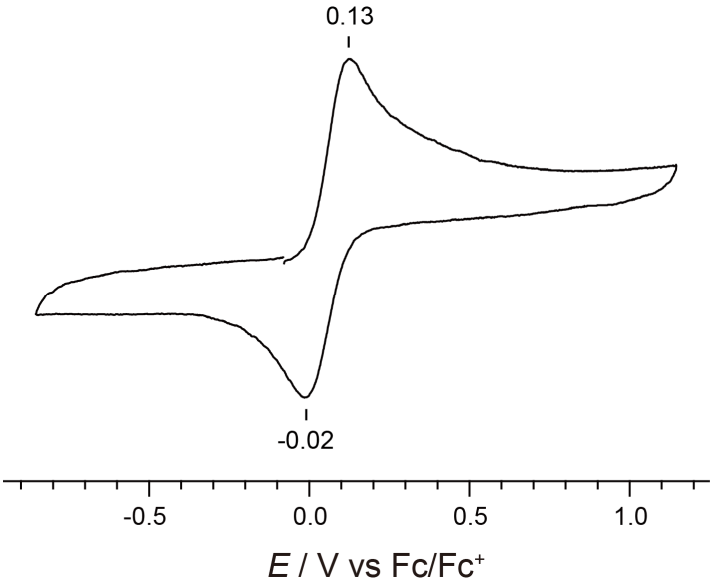

Figure S9. Cyclic voltammograms of 1 mM $[Pt_2Mn(piam)_4(NH_3)_4](PF_6)_2$ (**1**) in MeCN, with 0.1 M Bu_4NPF_6 as a supporting electrolyte using a glassy carbon disk working electrode, a Ag/Ag^+ reference electrode, and a Pt wire auxiliary electrode (scan rate 100 mV/s). Electrode potentials were converted to those relative to Fc/Fc^+.

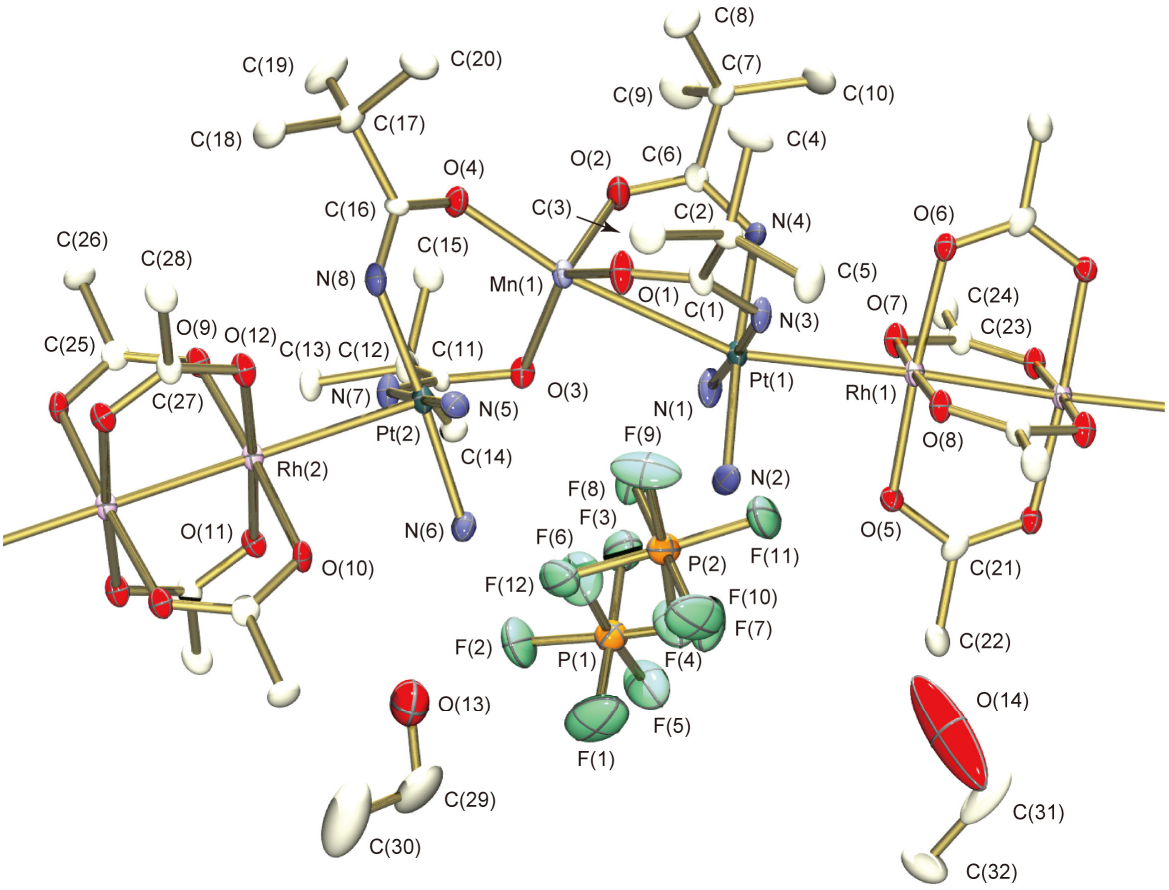

Figure S10. Crystal structure of [{$Rh_2(O_2CCH_3)_4$}{$Pt_2Mn(piam)_4(NH_3)_4$}]$_n(PF_6)_{2n}\cdot 1.5n$EtOH (**2**). The hydrogen atoms are omitted for clarity.

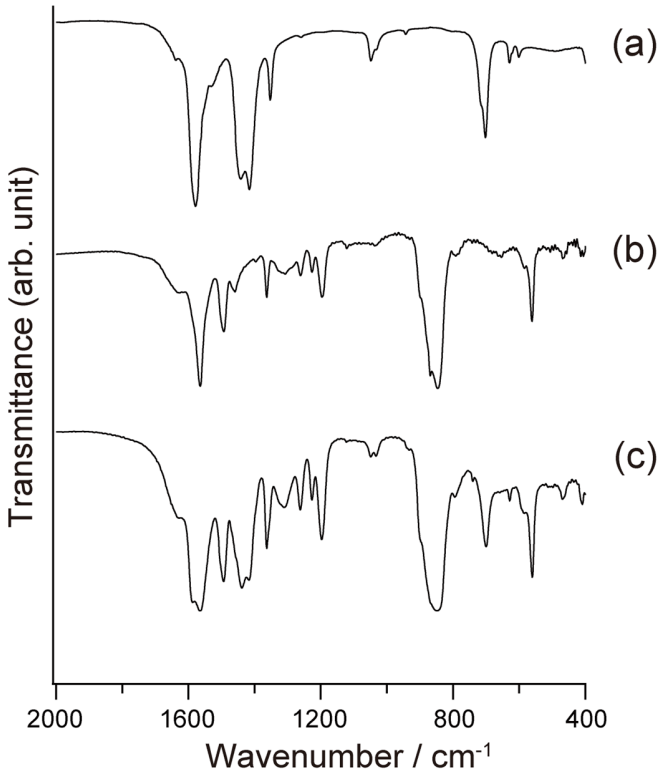

Figure S11. IR spectra (KBr pellet) of (a) [$Rh_2(O_2CCH_3)_4$], (b) [$Pt_2Mn(piam)_4(NH_3)_4$](PF_6)$_2$ (**1**), and (c) [{$Rh_2(O_2CCH_3)_4$}{$Pt_2Mn(piam)_4(NH_3)_4$}]$_n$(PF_6)$_{2n}$·1.5*n*EtOH (**2**) at room temperature.

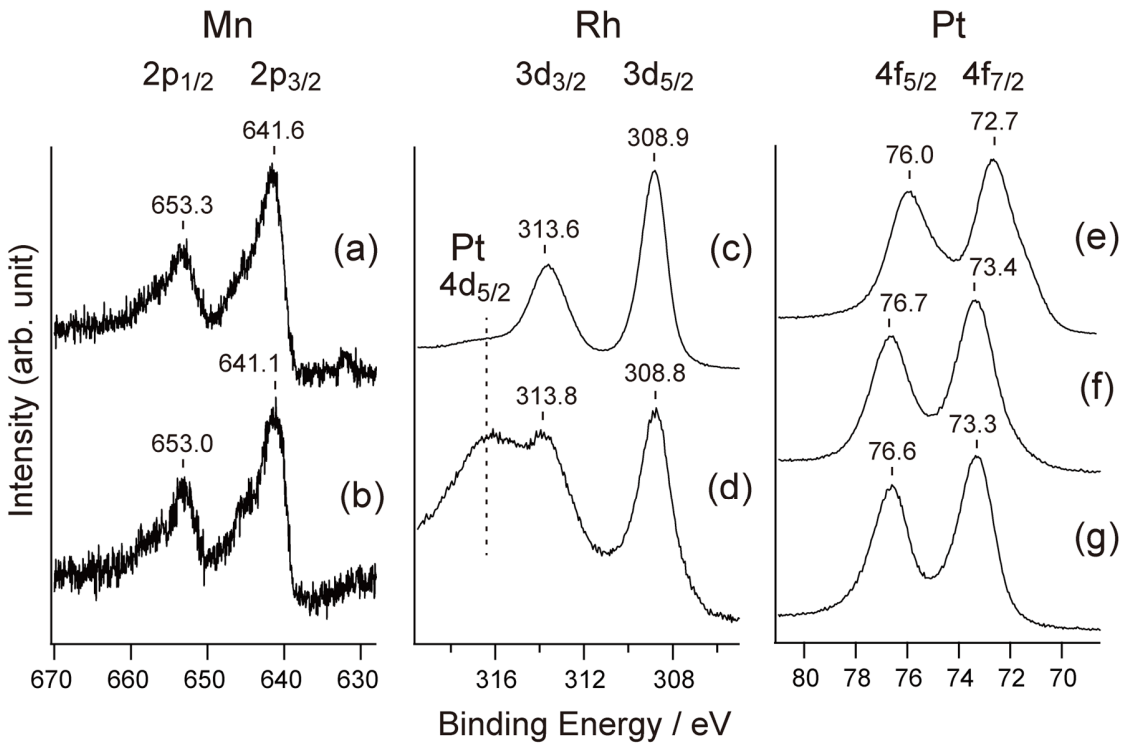

Figure S12. Mn $2p_{1/2}$ and $2p_{3/2}$, Rh $3d_{3/2}$ and $3d_{5/2}$, and Pt $4f_{5/2}$ and $4f_{7/2}$ core levels of XPS for (a) $[Pt_2Mn(piam)_4(NH_3)_4](PF_6)_2$ (**1**), (b) $[\{Rh_2(O_2CCH_3)_4\}\{Pt_2Mn(piam)_4(NH_3)_4\}]_n(PF_6)_{2n}\cdot 1.5n$EtOH (**2**), (c) $[Rh_2(O_2CCH_3)_4]$, (d) **2**, (e) *cis*-$[Pt(piam)_2(NH_3)_2]\cdot 2H_2O$, (f) **1**, and (g) **2**.

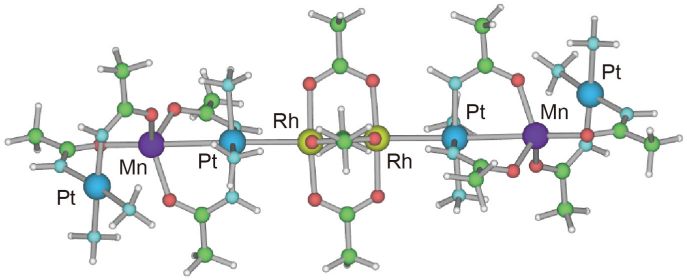

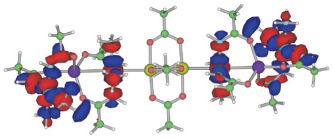

α LUMO+6

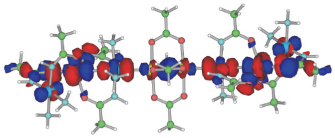

α HOMO

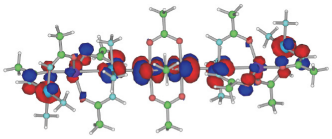

α HOMO-7

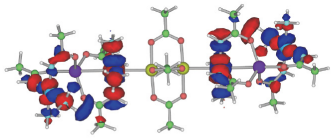

α LUMO+5

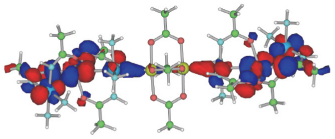

α HOMO-1

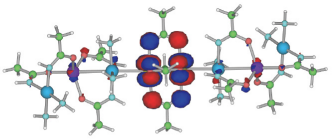

α HOMO-8

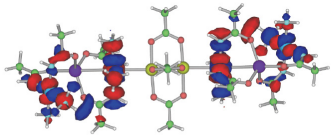

α LUMO+4

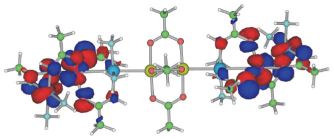

α HOMO-2

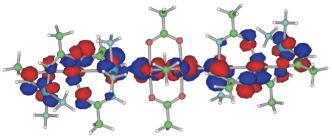

α HOMO-9

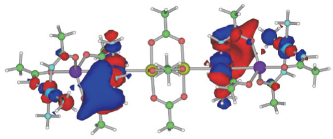

α LUMO+3

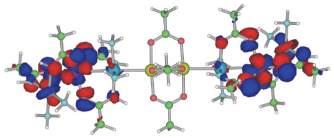

α HOMO-3

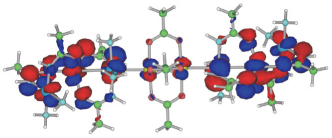

α HOMO-10

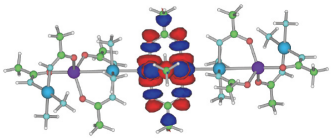

α LUMO+2

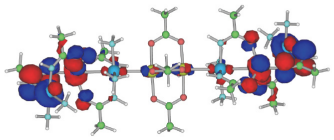

α HOMO-4

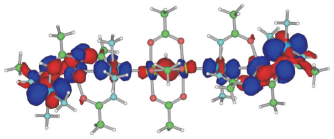

α HOMO-11

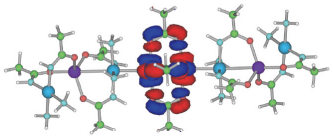

α LUMO+1

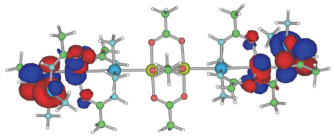

α HOMO-5

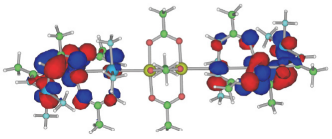

α HOMO-12

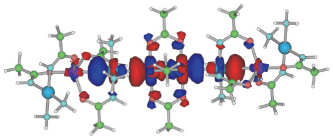

α LUMO

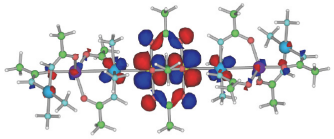

α HOMO-6

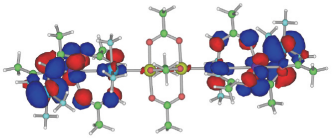

α HOMO-13

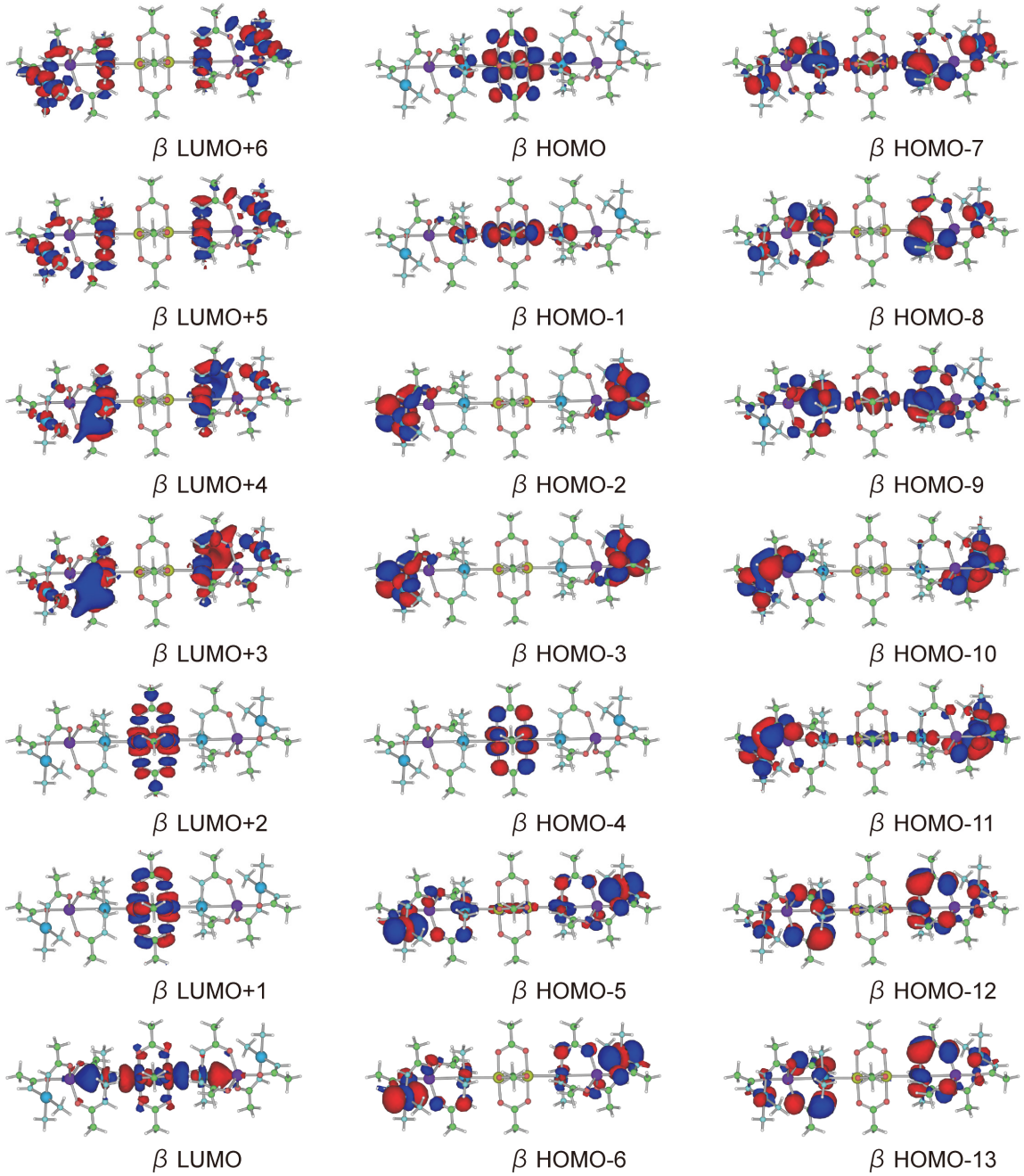

Figure S13. Result of DFT calculation of $[\{Rh_2(O_2CCH_3)_4\}\{Pt_2Mn(NHCOCH_3)_4(NH_3)_4\}_2]^{4+}$ (**1_{Td}-Rh_2-1_{Td}**).

Table S4. Optimized coordinates for $[\{Rh_2(O_2CCH_3)_4\}\{Pt_2Mn(NHCOCH_3)_4(NH_3)_4\}_2]^{4+}$ (**1_{Td}-Rh_2-1_{Td}**).

1	Pt	2.9335175	-0.3813679	-2.7003207
2	Pt	6.1334228	-2.6922067	-6.2394512
3	Rh	0.8354756	-0.1055243	-0.8504521
4	Mn	4.6894884	0.0411441	-5.1082016
5	O	2.0456227	1.136679	0.3038394
6	O	0.0385689	-1.5385252	1.7730149
7	O	0.4533204	1.3518544	1.8936322
8	O	1.6155492	-1.7467478	0.1792468
9	O	6.0283861	-0.7475657	-3.6472016
10	O	3.0770692	-1.1112924	-5.7919107
11	O	4.2780706	1.9145391	-4.4836908
12	O	5.7216407	0.541419	-6.7449667
13	N	2.4047357	1.4882205	-3.2891304
14	H	1.4971811	1.8328957	-2.9922614
15	N	4.7590868	-2.9578427	-7.8334369
16	H	3.9098555	-2.4519715	-7.5637755
17	H	4.5098696	-3.9096276	-8.1009632
18	H	5.1342731	-2.500257	-8.6658316
19	N	6.965803	-1.2486158	-7.3829485
20	H	7.7676118	-1.5284574	-7.9381607
21	N	3.3970972	-2.3302586	-1.9918209
22	H	4.3987131	-2.5114296	-1.9603568
23	H	2.9580619	-3.022569	-2.5966899
24	H	2.9869251	-2.4294976	-1.0553415
25	N	7.3873092	-2.2521275	-4.706983
26	H	8.3406419	-2.5981478	-4.7397577
27	N	1.6421733	-1.2115135	-4.0225804
28	H	0.6853271	-1.3828693	-3.7271699
29	N	5.4648514	-4.4071952	-5.1418949
30	H	5.8937059	-4.400205	-4.2164111
31	H	5.7947766	-5.2561832	-5.6054525
32	H	4.4573055	-4.5020392	-5.0252515
33	N	4.3823152	0.5175436	-1.4491648
34	H	5.3017804	0.2612837	-1.8241495
35	H	4.3022413	0.2698243	-0.4646506
36	H	4.2814526	1.5302899	-1.5059397
37	C	3.1532141	2.2930986	-4.0229855
38	C	1.9181096	-1.3536558	-5.3057734
39	C	1.6120668	1.5918444	1.4127617
40	C	7.1601821	-1.3459852	-3.7752693
41	C	6.6594423	0.038954	-7.4398888
42	C	8.2568966	-0.9918386	-2.7976639
43	H	8.5205294	0.0622883	-2.9297451
44	H	9.1576603	-1.5949848	-2.9218252
45	H	7.8948431	-1.1119682	-1.7721656
46	C	1.0514075	-2.1160293	1.2658349
47	C	2.6978671	3.6986169	-4.3217436
48	H	3.4702319	4.3991824	-3.992194
49	H	1.7496131	3.9529238	-3.8450571
50	H	2.6030326	3.8183554	-5.4048
51	C	2.5401651	2.4521296	2.2317013
52	H	1.9754454	3.1967005	2.7946636
53	H	3.2751704	2.945364	1.5950174
54	H	3.0739406	1.8193923	2.949722
55	C	1.6008871	-3.3253499	1.9759845
56	H	1.0986174	-4.2216794	1.5948154
57	H	1.411368	-3.2593902	3.0479721
58	H	2.6713847	-3.4308352	1.7942351
59	C	0.843215	-1.8340628	-6.2526896
60	H	0.676649	-1.0678879	-7.0157495

61	H	-0.1031753	-2.0477487	-5.7533753
62	H	1.1774722	-2.7377725	-6.7708197
63	C	7.4219767	0.9521159	-8.3660977
64	H	6.7165369	1.4331359	-9.049346
65	H	8.1903671	0.4383959	-8.9460055
66	H	7.8876158	1.7462917	-7.7755509
67	Pt	-2.9335175	0.3813679	2.7003207
68	Pt	-6.1334228	2.6922067	6.2394512
69	Rh	-0.8354756	0.1055243	0.8504521
70	Mn	-4.6894884	-0.0411441	5.1082016
71	O	-2.0456227	-1.136679	-0.3038394
72	O	-0.0385689	1.5385252	-1.7730149
73	O	-0.4533204	-1.3518544	-1.8936322
74	O	-1.6155492	1.7467478	-0.1792468
75	O	-6.0283861	0.7475657	3.6472016
76	O	-3.0770692	1.1112924	5.7919107
77	O	-4.2780706	-1.9145391	4.4836908
78	O	-5.7216407	-0.541419	6.7449667
79	N	-2.4047357	-1.4882205	3.2891304
80	H	-1.4971811	-1.8328957	2.9922614
81	N	-4.7590868	2.9578427	7.8334369
82	H	-3.9098555	2.4519715	7.5637755
83	H	-4.5098696	3.9096276	8.1009632
84	H	-5.1342731	2.500257	8.6658316
85	N	-6.965803	1.2486158	7.3829485
86	H	-7.7676118	1.5284574	7.9381607
87	N	-3.3970972	2.3302586	1.9918209
88	H	-4.3987131	2.5114296	1.9603568
89	H	-2.9580619	3.022569	2.5966899
90	H	-2.9869251	2.4294976	1.0553415
91	N	-7.3873092	2.2521275	4.706983
92	H	-8.3406419	2.5981478	4.7397577
93	N	-1.6421733	1.2115135	4.0225804
94	H	-0.6853271	1.3828693	3.7271699
95	N	-5.4648514	4.4071952	5.1418949
96	H	-5.8937059	4.400205	4.2164111
97	H	-5.7947766	5.2561832	5.6054525
98	H	-4.4573055	4.5020392	5.0252515
99	N	-4.3823152	-0.5175436	1.4491648
100	H	-5.3017804	-0.2612837	1.8241495
101	H	-4.3022413	-0.2698243	0.4646506
102	H	-4.2814526	-1.5302899	1.5059397
103	C	-3.1532141	-2.2930986	4.0229855
104	C	-1.9181096	1.3536558	5.3057734
105	C	-1.6120668	-1.5918444	-1.4127617
106	C	-7.1601821	1.3459852	3.7752693
107	C	-6.6594423	-0.038954	7.4398888
108	C	-8.2568966	0.9918386	2.7976639
109	H	-8.5205294	-0.0622883	2.9297451
110	H	-9.1576603	1.5949848	2.9218252
111	H	-7.8948431	1.1119682	1.7721656
112	C	-1.0514075	2.1160293	-1.2658349
113	C	-2.6978671	-3.6986169	4.3217436
114	H	-3.4702319	-4.3991824	3.992194
115	H	-1.7496131	-3.9529238	3.8450571
116	H	-2.6030326	-3.8183554	5.4048
117	C	-2.5401651	-2.4521296	-2.2317013
118	H	-1.9754454	-3.1967005	-2.7946636
119	H	-3.2751704	-2.945364	-1.5950174
120	H	-3.0739406	-1.8193923	-2.949722
121	C	-1.6008871	3.3253499	-1.9759845
122	H	-1.0986174	4.2216794	-1.5948154
123	H	-1.411368	3.2593902	-3.0479721
124	H	-2.6713847	3.4308352	-1.7942351

125	C	-0.843215	1.8340628	6.2526896
126	H	-0.676649	1.0678879	7.0157495
127	H	0.1031753	2.0477487	5.7533753
128	H	-1.1774722	2.7377725	6.7708197
129	C	-7.4219767	-0.9521159	8.3660977
130	H	-6.7165369	-1.4331359	9.049346
131	H	-8.1903671	-0.4383959	8.9460055
132	H	-7.8876158	-1.7462917	7.7755509

Table S5. Comparison of selected distances (Å) and angles (°) between $[\{Rh_2(O_2CCH_3)_4\}\{Pt_2Mn(piam)_4(NH_3)_4\}]_n(PF_6)_{2n}\cdot 1.5n$EtOH (**2**) and $[\{Rh_2(O_2CCH_3)_4\}\{Pt_2Mn(NHCOCH_3)_4(NH_3)_4\}_2]^{4+}$ (**1_{Td}-Rh_2-1_{Td}**).

Compounds	Pt–Mn (Å)	Pt–Mn–Pt (°)	Mn–O (Å) O–Mn–O (°)
2	3.0099(12), 3.2927(11)	114.45(7)	2.040(7), 2.058(7), 2.066(6), 2.035(6) 100.1(3), 97.6(3), 114.0(3), 106.0(2), 132.1(3), 101.6(3)
1_{Td}-Rh_2-1_{Td}	3.0100, 3.2918	114.4727	1.9987, 2.0171, 2.1329, 2.0965 105.0340, 109.2286, 120.1923, 97.2619, 117.0401, 105.5274

Compounds	Rh–Rh (Å)	Rh–Rh–Pt (°)	Rh–Pt (Å)	Rh–Pt–Mn (°)	O–Rh–Pt–N (°) [a]
2	2.3937(11)	175.88(4)	2.8108(6)	161.47(3)	31
1_{Td}-Rh_2-1_{Td}	2.3937	175.8718	2.8107	161.4785	14

[a] Average of four angles.

Analyses of magnetic susceptibility measurements.

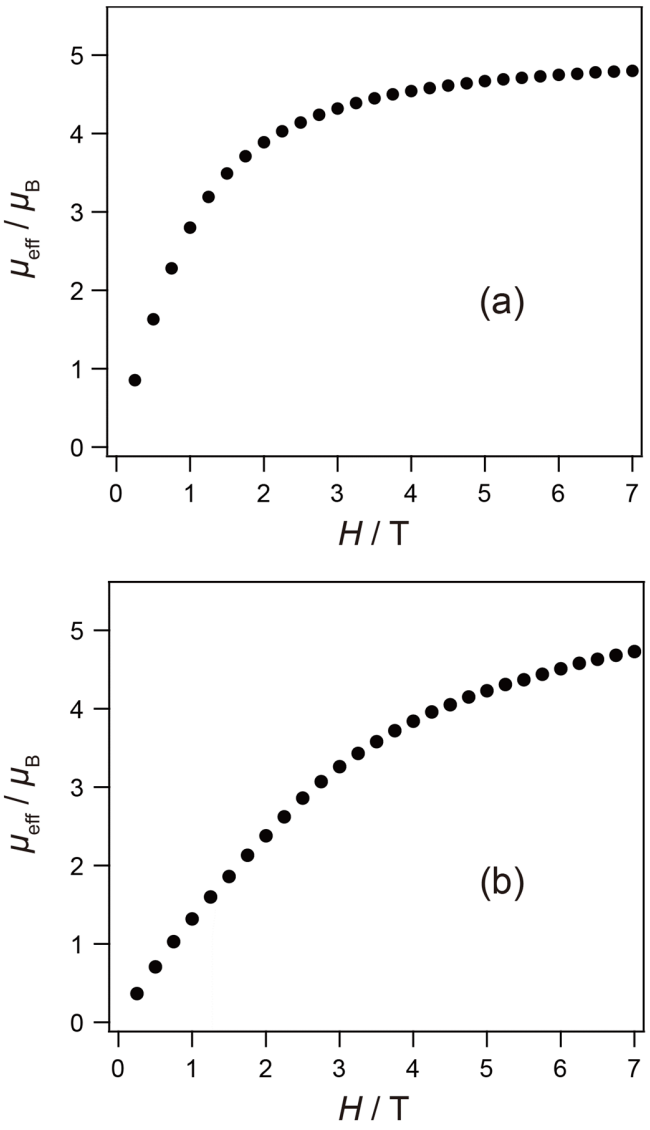

Figure S14. Magnetization curves against field at 2 K for (a) $[Pt_2Mn(piam)_4(NH_3)_4](PF_6)_2$ (**1**) and (b) $[\{Rh_2(O_2CCH_3)_4\}\{Pt_2Mn(piam)_4(NH_3)_4\}]_n(PF_6)_{2n}\cdot 1.5n$EtOH (**2**).

The data for **1** and **2** were fitted to the Curie–Weiss law $\chi = C/(T - \theta)$. The resulting least-squares fit between 30 K and 300 K yielded **1**: $C = 4.42$ cm^3 K mol^{-1} and $\theta = -0.40$ K, **2**: $C = 5.53$ cm^3 K mol^{-1} and $\theta = -11.55$ K (Figure S15). $C = N\beta^2g^2S(S + 1)/3k$, where N is Avogadro constant, β is the Bohr magneton, g is the Lande value, k is Boltzmann constant, θ is the Weiss constant, as the combination of constants $3k/N\beta^2$ is 7.991, gives **1**: $g = 2.01$, **2**: $g = 2.25$.

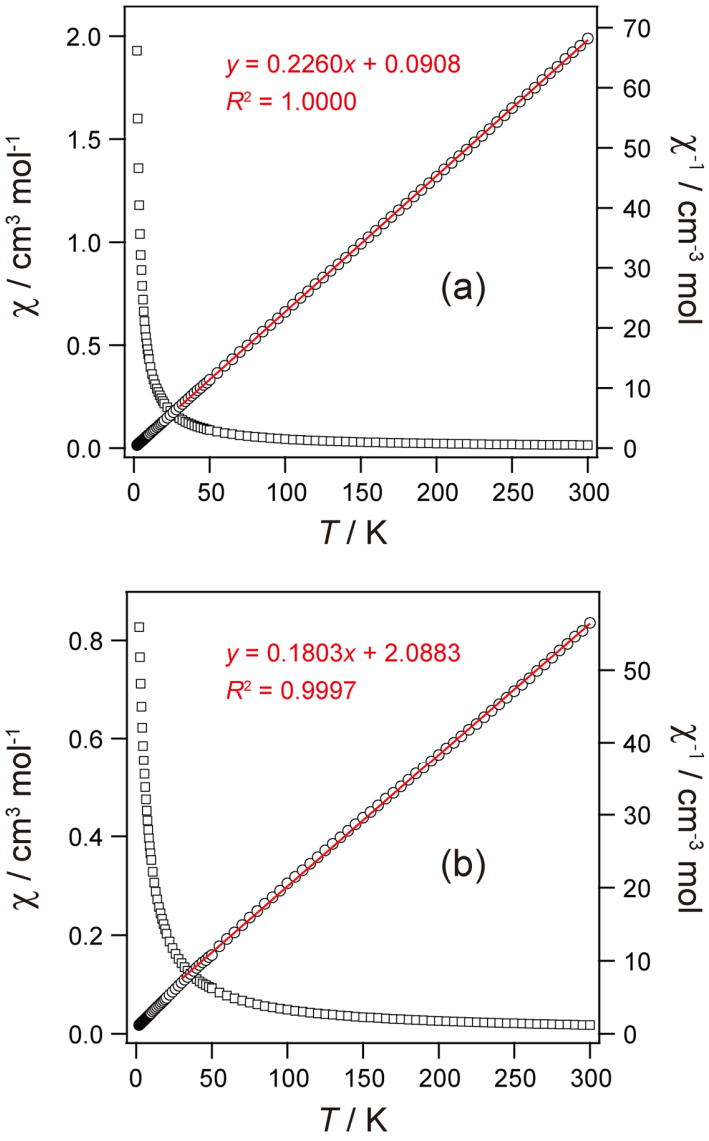

Figure S15. Temperature dependence of χ (square) and χ^{-1} (circle) for (a) $[Pt_2Mn(piam)_4(NH_3)_4](PF_6)_2$ (**1**) and (b) $[\{Rh_2(O_2CCH_3)_4\}\{Pt_2Mn(piam)_4(NH_3)_4\}]_n(PF_6)_{2n}\cdot 1.5n$EtOH (**2**). The red solid line represents the result of least square fitting.

The equations describing the temperature dependence of the molar magnetic susceptibility of a sextet state undergoing an axial ZFS are

$$\chi_{\parallel} = \frac{Ng^2\beta^2}{4kT}\frac{1 + 9exp\left(\frac{-2D}{kT}\right) + 25exp\left(\frac{-6D}{kT}\right)}{1 + exp\left(\frac{-2D}{kT}\right) + exp\left(\frac{-6D}{kT}\right)}$$

$$\chi_{\perp} = \frac{Ng^2\beta^2}{8kT}\frac{18 + \frac{kT}{D}\left(16 - 11exp\left(\frac{-2D}{kT}\right) - 5exp\left(\frac{-6D}{kT}\right)\right)}{1 + exp\left(\frac{-2D}{kT}\right) + exp\left(\frac{-6D}{kT}\right)}$$

where D is axial zero-field splitting parameter, k is Boltzmann constant, T is temperature, N is Avogadro constant, g is g-factor, and β is the Bohr magneton.[1] The average molar magnetic susceptibility of a powdered sample is given by

$$\chi' = \frac{\chi_{\parallel} + 2\chi_{\perp}}{3} + \text{TIP}$$

where TIP is the temperature independent paramagnetism. In some cases, it was necessary to include the contribution of an impurity present in a proportion P and which was assumed to follow a Curie law with $S = 1/2$ and a g factor noted as g_{mo} (fixed as 2.00). The complete expression of the magnetic susceptibility used for the refinements was therefore

$$\chi = (1 - P)\chi' + P\frac{Ng_{\text{mo}}^2\beta^2}{4kT}$$

According the above equation, the resulting least-squares fit of the data of **1** between 2 K and 300 K yielded $g = 2.00$, $D = 1.21$ cm^{-1}, TIP = 0.00 cm^3 mol^{-1}, and $P = 1.00 \times 10^{-4}$ (Figure S16).

In order to estimate the intermolecular interaction, the molecular field approximation may be used with the following analytical expression

$$\chi'' = \frac{\chi'}{1 - \left(\frac{2zJ}{Ng^2\beta^2}\right)\chi'}$$

where zJ is the exchange energy (J multiplied by the number z of interacting neighbors), and χ' is the magnetic susceptibility of an isolated molecules, resulting from previous equation. Similarly, the

contribution of a paramagnetic impurity was included to yield the complete expression used for the refinements

$$\chi = (1 - P)\chi'' + P\frac{Ng_{\mathrm{mo}}^2\beta^2}{4kT}$$

According the above equation, the resulting least-squares fit of the data of **1** between 2 K and 300 K yielded $g = 2.00$, $D = 1.02$ cm^{-1}, $zJ = -0.01$ cm^{-1}, TIP = 0.00 cm^3 mol^{-1}, and $P = 1.02 \times 10^{-4}$ (Figure S17).

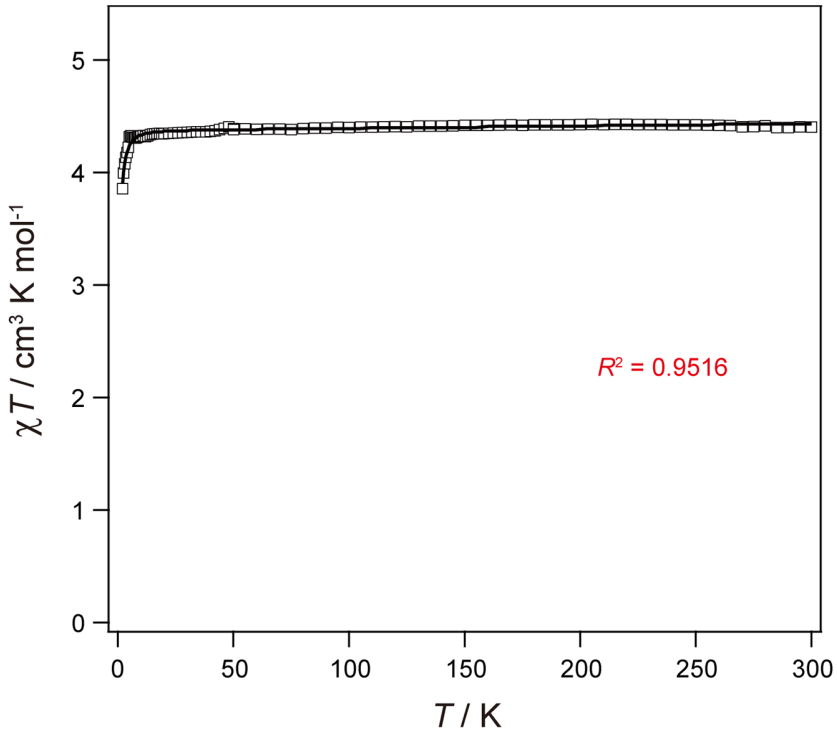

Figure S16. Temperature dependence of χT (square) for $[Pt_2Mn(piam)_4(NH_3)_4](PF_6)_2$ (**1**) per Mn ion. The solid line represents the theoretical fitting to the axial ZFS model for sextet state.

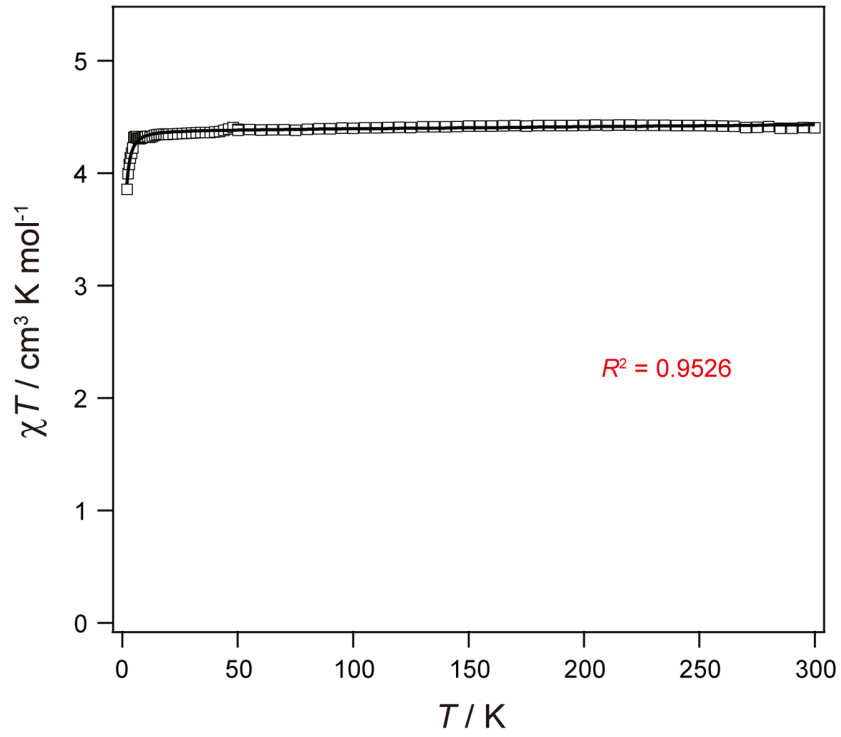

Figure S17. Temperature dependence of χT (square) for $[Pt_2Mn(piam)_4(NH_3)_4](PF_6)_2$ (**1**) per Mn ion. The solid line represents the theoretical fitting to the axial ZFS model for sextet state with the molecular field approximation.

The susceptibility data of **2** was fitted to the expression for the molar susceptibility derived from $H = -2JS_1 \cdot S_2$.[1]

$$\chi = \frac{Ng^2\beta^2}{kT} \frac{55 + 30x^{10} + 14x^{18} + 5x^{24} + x^{28}}{11 + 9x^{10} + 7x^{18} + 5x^{24} + 3x^{28} + x^{30}} + \text{TIP}$$

$$x = exp\left(\frac{-J}{kT}\right)$$

where J represents the exchange interactions between two adjacent Mn(+2) centers. According the above equation, the resulting least-squares fit of the data of **2** between 2 K and 300 K yielded $J = -0.26$ cm^{-1} and $g = 2.04$ (Figure S18).

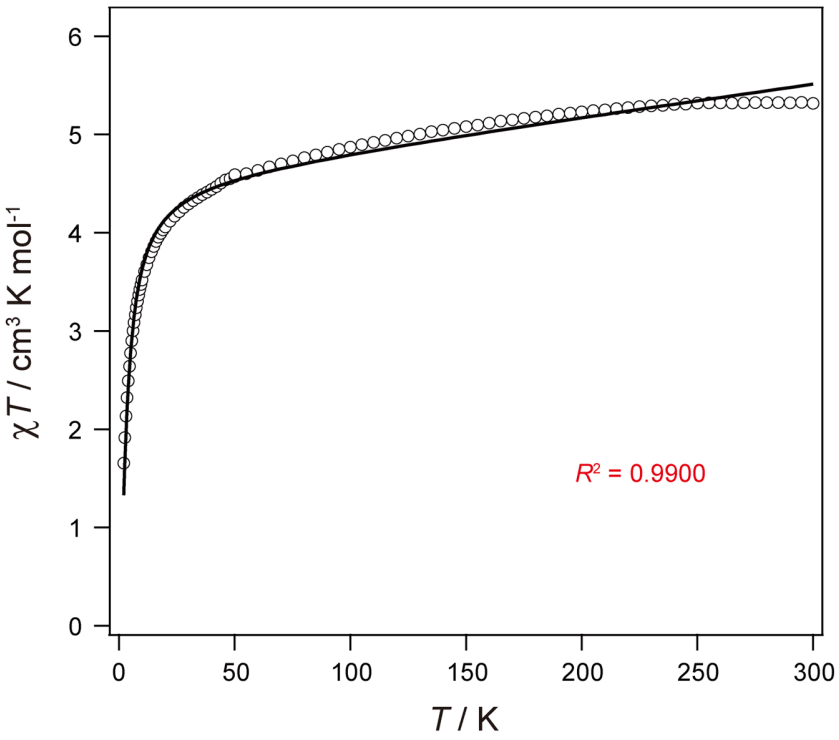

Figure S18. Temperature dependence of χT (circle) for $[\{Rh_2(O_2CCH_3)_4\}\{Pt_2Mn(piam)_4(NH_3)_4\}]_n(PF_6)_{2n} \cdot 1.5n$EtOH (**2**) per Mn ion. The solid line represents the theoretical fitting to the above expression for the molar susceptibility derived from $H = -2JS_1 \cdot S_2$.

The susceptibility data of **2** was fitted to the Fisher's equation[2] and Wagner-Friedberg model[3] for infinite chains.

$$\chi = \frac{Ng^2\beta^2}{3kT}\, S(S+1)\frac{(1+u)}{(1-u)}$$

where $S = 5/2$ and u is

$$u = coth\left[\frac{2JS(S+1)}{kT}\right] - \left[\frac{kT}{2JS(S+1)}\right]$$

and J represents the exchange interactions between two adjacent Mn(+2) centers. According the above equation, the resulting least-squares fit of the data of **2** between 2 K and 300 K yielded $J = -0.21$ cm^{-1} and $g = 2.17$ (Figure S19).

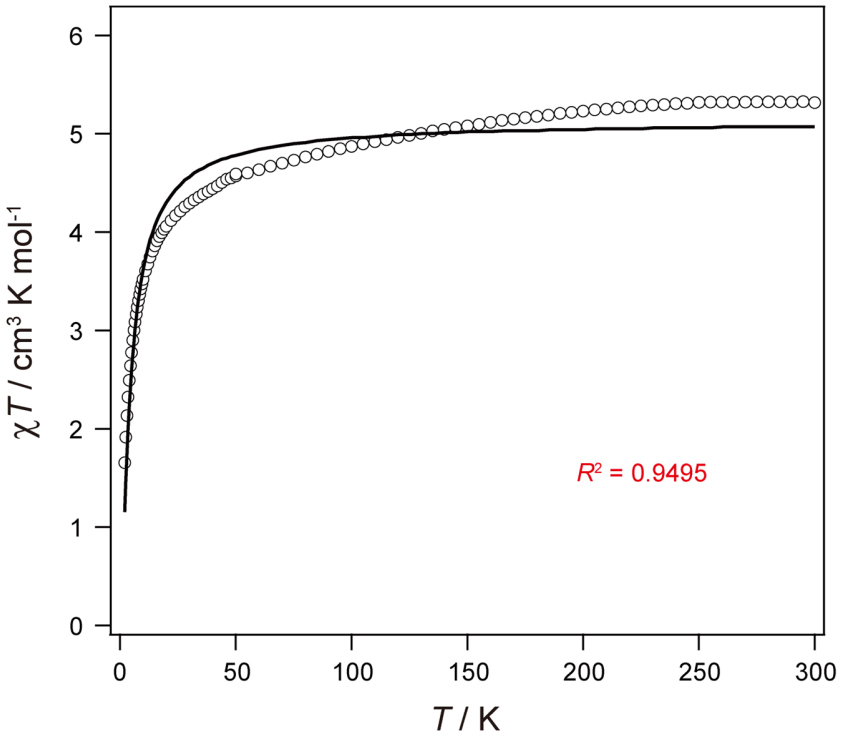

Figure S19. Temperature dependence of χT (circle) for $[\{Rh_2(O_2CCH_3)_4\}\{Pt_2Mn(piam)_4(NH_3)_4\}]_n(PF_6)_{2n}\cdot 1.5n$EtOH (**2**) per Mn ion. The solid line represents the theoretical fitting to the Fisher and Wagner-Friedberg model.

The susceptibility data of **2** was fitted to the Weng's numerical model.[4,5]

$$\chi = \frac{Ng^2\beta^2}{kT}\left(\frac{2.9167 + 208.04(|J|/kT)^2}{1 + 15.543(|J|/kT) + 2707.2(|J|/kT)^3}\right)$$

According the above equation, the resulting least-squares fit of the data of **2** between 2 K and 300 K yielded $J = -0.20$ cm^{-1} and $g = 2.18$ (Figure S20).

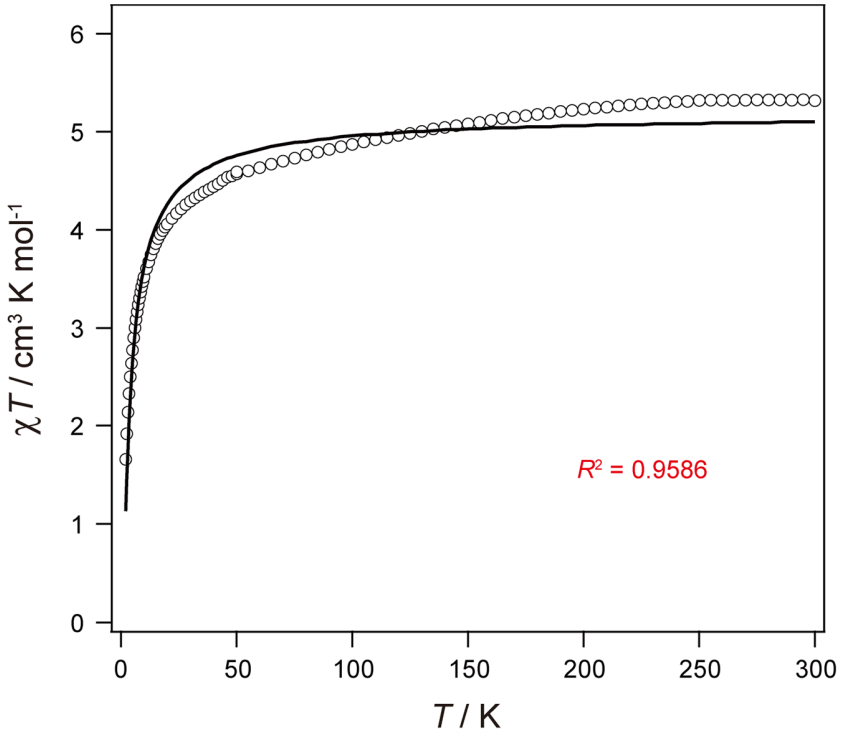

Figure S20. Temperature dependence of χT (circle) for $[\{Rh_2(O_2CCH_3)_4\}\{Pt_2Mn(piam)_4(NH_3)_4\}]_n(PF_6)_{2n}\cdot 1.5n$EtOH (**2**) per Mn ion. The solid line represents the theoretical fitting to the Weng's model.

According to the theoretical fitting to the axial ZFS model for sextet state with the molecular field approximation, the resulting least-squares fit of the data of **2** between 2 K and 300 K yielded $g = 2.09$, $D = 1.21\ cm^{-1}$, $zJ = -0.43\ cm^{-1}$, TIP = 0.00 $cm^3\ mol^{-1}$, and $P = 1.03 \times 10^{-4}$ (Figure S21).

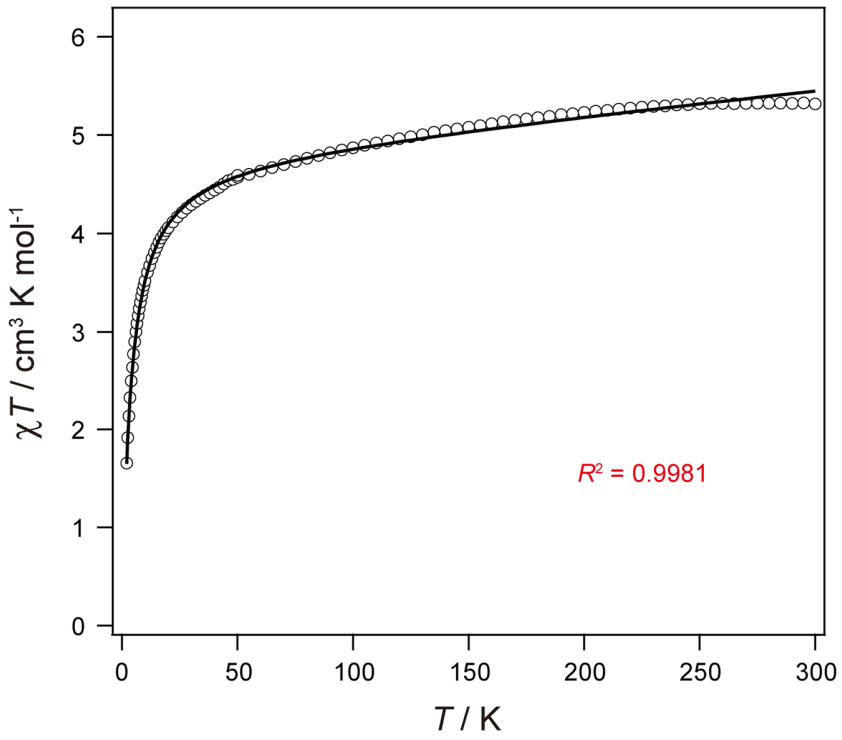

Figure S21. Temperature dependence of χT (circle) for $[\{Rh_2(O_2CCH_3)_4\}\{Pt_2Mn(piam)_4(NH_3)_4\}]_n(PF_6)_{2n}\cdot 1.5n$EtOH (**2**) per Mn ion. The solid line represents the theoretical fitting to the axial ZFS model for sextet state with the molecular field approximation.

(1) Kahn, O., *Molecular Magnetism*; VCH Publishers Inc.: New York, 1993.
(2) Fisher, M. E., *Am. J. Phys.* **1964,** *32*, 343–346.
(3) Wagner, G. R.; Friedberg, S. A., *Phys. Lett.* **1964,** *9*, 11–13.
(4) Weng, C. H., Ph.D. Dissertation, Carnegie-Mellon University, Pittsburgh, PA, 1968.
(5) Hiller, W.; Strähle, J.; Datz, A.; Hanack, M.; Hatfield, W. E.; Haar, L. W. t.; Gütlich, P., *J. Am. Chem. Soc.* **1984,** *106*, 329–335.

Table S6. The distances (Å) of Mn---Mn and J values (cm^{-1}) in reported 1D compounds shown in Figure 11.

Compounds	Mn---Mn (Å)	J (cm^{-1})	ref
Mn atoms are bridged by organic molecules or halide ions			
$[Mn(L)(pyz)]_n(ClO_4)_n \cdot 2nH_2O$	3.244	−0.95	62
$[(CH_3)_4N]_n[MnCl_3]_n$	3.25	−4.38	63
$[MnL'(N_3)_2]_n$	3.462	−2.66	64
$[MnCl_2]_n \cdot 2nH_2O$	3.7	−0.31	65
$[Mn(\mu\text{-}Cl)_2(mppma)]_n$	3.7398	−0.13	66
$[Mn_2(tpa)_2(o\text{-}phth)]_n(ClO_4)_{2n}$	4.452	−1.2	67
$[Mn(\mu\text{-}3\text{-}ClPhCOO)_2(bpy)]_n \cdot nH_2O$	4.515	−0.86	68
$[Mn(\mu\text{-}ClCH_2COO)_2(phen)]_n$	4.53	−0.45	69
$(CH_3NH_3)_n[MnCl_3]_n \cdot 2nH_2O$	4.599	−2.09	70
$[Mn_2(bipy)_4(ta)]_n(ClO_4)_{2n}$	4.643	−0.675	71
$[Mn(PDB)]_n \cdot nH_2O$	4.8	−0.28	72
$[Mn_2(bipy)_4(m\text{-}phth)]_n(ClO_4)_{2n} \cdot 4nH_2O$	4.84	−0.49	73
$[Mn\{(CH_3)_2PO_2\}_2]_n$	4.8652	−2.94	74
$[Mn(bic)Cl]_n \cdot nH_2O$	4.987	−0.30	75
$[Mn(bpy)(NCS)_2]_n$	6	−1.35	54
$[Mn_2(EDTA)]_n \cdot 9nH_2O$	6.1	−0.25	76
$[Mn_2(bpym)_3(tcpd)_2(H_2O)_2]_n$	6.13	−0.58	77
$[Mn(CH_3CONH_2)_2(HPhPO_2)_2]_n$	7.43	−0.30	78
$[Mn(HPhPO_2H)_2(HPhPO_2)_2]_n$	7.43	−0.13	78
$[Mn(MAC)\{\mu_{1.5}\text{-}NN(CN)_2\}]_n(PF_6)_n$	7.7	−0.25	79
$[Mn(C_5H_6NO_3)_2]_n$	7.963	−0.38	80
$[Mn(tpa)(TCNQ)(CH_3OH)]_n(TCNQ)_{2n} \cdot nCH_3CN$	8.207	−0.972	57
$[Mn(MAC)(H_2O)_2]_nCl_{2n} \cdot 4nH_2O$	13.03	−0.09	81
Mn atoms are bridged by second metals.			
$[MnNiMn(dpa)_4Cl_2]$	5.25	−6.85	82
$[MnPdMn(dpa)_4Cl_2]$	5.28	−14.85	82
$[MnPtMn(dpa)_4Cl_2]$	5.26	−33.1	82
2	13.9	−0.43	this work

Abbreviation: HL = Schiff base ligand, pyz = pyrazine, L' = (E)-3-(dimethylamino)-1-(pyridin-2-yl)prop-2-en-1-one), mppma = *N*-(3-methoxypropyl)-*N*-(pyridin-2-ylmethyl)amine, tpa = tris(2-pyridylmethyl)amine, *o*-phth = terephthalato dianion, phen = phenanthroline, H_2PDB = pyridine-3,4-dicarboxylic acid, *m*-phth = isophthalate, bic = bicinate, bpy = 2,2'-bipyridine, EDTA = ethylenediaminetetraacetic acid, bpym = 2,2'-bipyrimidine, tcpd = 2-dicyanomethylene-1,1,3,3-tetracyanopropanediide anion, MAC = 2,13-dimethyl-3,6,9,12,18-pentaazabicyclo-[12.3.1]octadeca-1(18),2,12,14,16-pentaene, TCNQ = tetracyanoquinodimethane, Hdpa = dipyridylamine.